LIQUID-SHEET SPRAY COOLING FROM CONVERGENT MICRONOZZLES: SPATIALLY RESOLVED HEAT TRANSFER MEASUREMENTS

Arpan Sow, Alexandros Peteinaris and Alexandros Terzis

Thermo-Fluids & Interfaces Lab
The Stephen B. Klein Faculty of Aerospace Engineering
Technion – Israel Institute of Technology, 3200003 Haifa, Israel

E-mail: aterzis@technion.ac.il

ABSTRACT

Liquid-sheet spray cooling offers a promising approach for high-heat-flux thermal management in ultra-confined geometries; however, its spatially varying heat-transfer behavior remains poorly characterized. This work presents a steady-state inverse-conduction method for reconstructing the local wetted-surface temperature, convective heat flux, and heat-transfer coefficient from backside infrared measurements of a Joule-heated multilayer thermal stack. Validation using Inconel 600 and Constantan heater foils under round air-jet impingement demonstrates consistent Nusselt-number distributions across different foil materials and imposed heat-flux levels. When applied to a planar water-sheet spray, the method reveals strongly non-axisymmetric cooling patterns governed by sheet stability, breakup behavior, and droplet trajectories. Stable liquid sheets produce broad and relatively uniform cooling footprints, whereas sheet breakup concentrates heat transfer within localized droplet-impingement regions.

INTRODUCTION

Microfluidic convergent nozzles can generate thin liquid sheets that subsequently atomize into planar sprays with controllable geometry, thickness, and droplet-size distribution [1–4]. Their narrow spray geometry is particularly attractive for cooling ultra-confined regions in compact energy-conversion, electronic, and aerospace systems, where conventional conical sprays may be geometrically restricted. However, liquid-sheet sprays are strongly anisotropic and non-axisymmetric, with cooling footprints governed by sheet breakup, droplet trajectories, and local mass-flux distributions.

Reliable characterization of these cooling footprints requires spatially resolved measurements of the surface temperature, heat flux, and heat-transfer coefficient. Infrared thermography provides full-field temperature data; however, the wetted-surface conditions must generally be reconstructed from backside or subsurface temperature measurements using an inverse heat-conduction analysis [5,6]. Existing methods often rely on iterative numerical inversion or symmetry assumptions that are not well suited to planar sprays.

The present study introduces a steady-state inverse-conduction method based on backside infrared imaging of a Joule-heated multilayer thermal stack. The method accounts for through-thickness conduction, lateral heat spreading, and local backside heat losses, enabling reconstruction of the wetted-surface temperature, convective heat flux, and heat-transfer coefficient without iterative inversion. The approach is validated using round air-jet impingement and subsequently applied to microfluidic liquid-sheet sprays, demonstrating its ability to resolve strongly non-axisymmetric surface-temperature, heat-flux, and heat-transfer-coefficient fields.

MATERIALS AND METHODS

Heat transfer model

Figure 1 shows the multilayer thermal stack used to reconstruct the local wetted-surface temperature and heat-transfer coefficient. The assembly comprised a 25-µm-thick metallic foil bonded to 1-mm-thick soda-lime glass

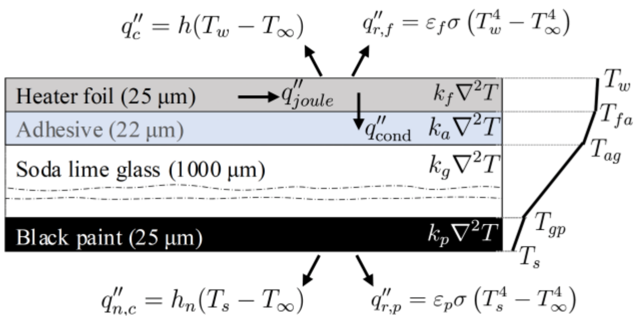

Figure 1. Schematic of the multilayer thermal stack and energy balance. A metallic foil is bonded to soda-lime glass using a thin acrylic adhesive layer. The backside of the glass is coated with high-emissivity black paint and imaged using an IR camera to obtain the steady-state temperature field. The electrical heat input, q''_{joule}, together with the conduction model, $q''_{\text{cond}}(x,y)$, is used to reconstruct the wetted-surface temperature, $T_w(x, y)$, and the local convective heat flux, $q''_c(x, y)$.

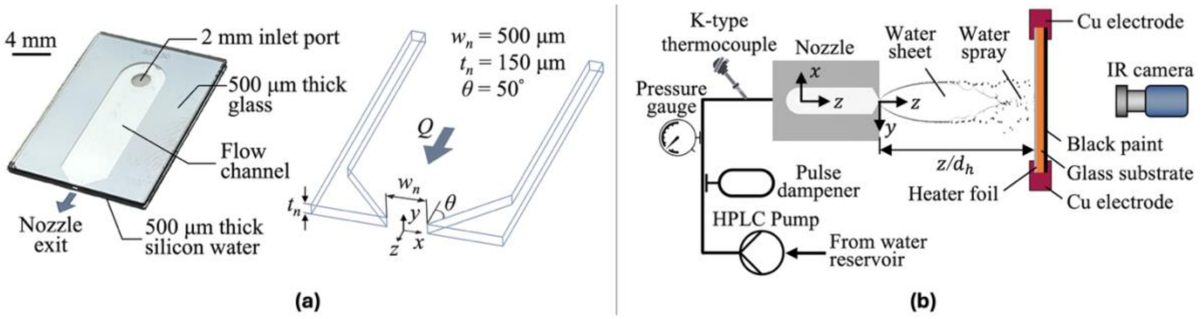

Figure 2. (a) Convergent silicon-glass microfluidic nozzle used to generate the planar water-sheet spray. The device consists of a 500 µm-thick silicon wafer containing the etched converging microchannel, anodically bonded to a 500 µm-thick glass cover. The rectangular outlet has width w_n = 500 µm, thickness t_n = 150 µm, and convergence angle θ = 50°. **(b)** Spray-cooling setup. Deionized water is supplied from a reservoir through an in-line pulse dampener to the nozzle, where a planar sheet is formed and subsequently atomizes before impinging on the Joule-heated multilayer target. The painted backside is monitored by an IR camera.

using a thin acrylic adhesive layer. The backside of the glass was coated with high-emissivity black paint. Inconel 600 and Constantan foils were tested independently to assess the sensitivity of the method to the heater material.

Under uniform Joule heating and steady-state conditions, the backside temperature field, $T_s(x,y)$, was obtained by averaging 1000 infrared frames. The local convective heat flux was calculated from the surface energy balance

$$q''_c = q''_{joule} - q''_{r,w} - q''_{cond},$$

where q''_{joule} = VI/A_{foil} and $q''_{r,w}$ is the radiative loss from the wetted foil. Conductive heat transfer through the multilayer stack was evaluated as

$$q''_{cond} = q''_b - S\,\nabla^2_{\perp} T_s, \quad S = \Sigma_i\, k_i t_i,$$

thereby accounting for both locally calibrated backside convection and radiation, q''_b, and lateral heat spreading. The wetted-surface temperature was reconstructed using

$$T_w = T_s + q''_{cond} R_{th}, \quad R_{th} = \Sigma_i\, t_i/k_i.$$

Finally, the local heat-transfer coefficient was obtained from $h = q''_c/(T_w - T_{ref})$. where the measured upstream water temperature was used for spray cooling.

Microfluidic nozzle and experimental setup

A silicon-glass microfluidic nozzle, shown in Figure 2a, generated the planar water-sheet spray. The device comprised a 50° convergent channel terminating in a 500 × 150 µm² rectangular outlet, corresponding to a hydraulic diameter of 230.7 µm. As shown in Figure 2b, deionized water was supplied from a reservoir by an HPLC pump through an in-line pulse dampener, while upstream pressure and spray temperature were monitored. Flow rates of 80–120 mL/min produced Reynolds numbers of 5600-10000 and Weber numbers of 490-1580. The spray atomized over a 96.5-mm nozzle-to-target distance before impinging on the Joule-heated multilayer target, whose backside temperature field was measured using infrared thermography.

RESULTS AND DISCUSSION

Figure 3 links the evolution of the water-sheet breakup morphology to the corresponding local heat-transfer-coefficient distributions for three Reynolds numbers.

At Re_d=3870, the primary sheet remains largely coherent until the rims merge near the sheet apex. Breakup is therefore dominated by droplets shed from the rims, producing a broad triangular spray. Consistently, the heat-transfer map shows an elongated cooling footprint along the *x*-direction, with multiple moderately enhanced regions and a comparatively uniform distribution over the wetted area.

At Re_d =4835, the rim inertia becomes sufficiently large for the rims and sheet to disintegrate independently. Droplets generated by both mechanisms converge toward the longitudinal axis after breakup, concentrating the spray near the centerline. The corresponding heat-transfer field contracts into a compact central region, with a single dominant maximum slightly displaced from the geometric center. This pattern indicates that droplet focusing, rather than the increase in flow rate alone, controls the local cooling intensity.

At Re_d =5800, breakup begins earlier, near the location of maximum sheet width. The two rims detach and propagate along nearly parallel trajectories, while stronger interfacial instabilities increase ligament formation and the fine-droplet fraction. The heat-transfer distribution consequently separates into two pronounced peaks located symmetrically about the nozzle axis, directly reflecting the impact locations of the rim-derived droplet streams.

Overall, the findings show a clear one-to-one relationship between sheet breakup, droplet trajectories, and surface-cooling topology. Increasing Reynolds number does not merely amplify heat transfer; it fundamentally reorganizes the spatial footprint from elongated, to centrally focused, and finally to distinctly two-lobed.

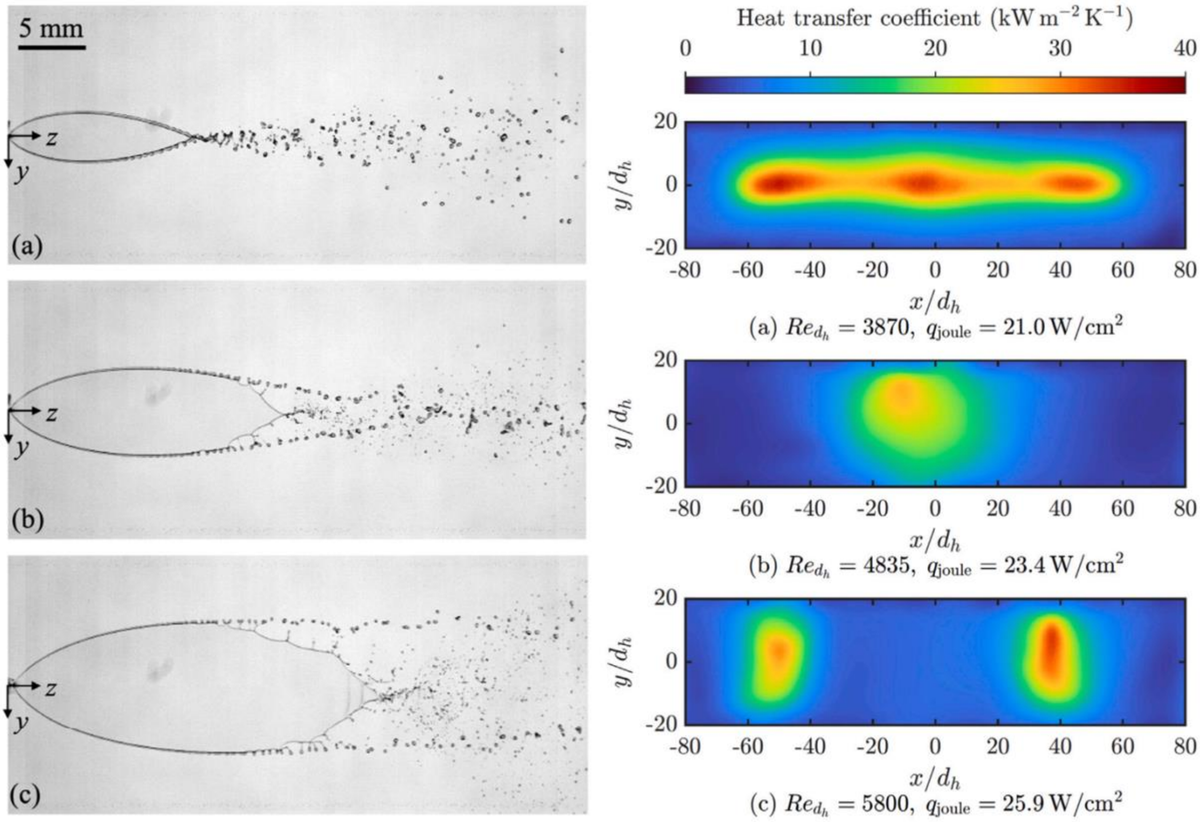

Figure 3. Coupled evolution of the water-sheet spray morphology and the corresponding local heat-transfer-coefficient distribution for increasing Reynolds number. (**Left**) Instantaneous shadowgraph images of the liquid sheet and downstream atomization region. (**Right**) Reconstructed surface maps of the local heat-transfer coefficient. At **(a)** Re_d=3870, the sheet remains largely coherent until near the apex, producing a broad, elongated cooling footprint dominated by rim-derived droplets. At (b) Re_d=4835, independent breakup of the sheet and rims causes droplets to converge toward the spray centerline, generating a compact region of enhanced heat transfer. At **(c)** Re_d=5800, earlier rim detachment produces two nearly parallel droplet streams and a corresponding two-lobed heat-transfer pattern. The imposed Joule heat fluxes are 21, 23.4, and 25.9 W/cm^2, respectively. Surface coordinates are normalized by the nozzle hydraulic diameter, *d*.

REFERENCES

1. Peteinaris, A., Sinha, P., Schmid, J. and Terzis, A. Morphology and dynamics scaling of water sheet jets generated by microfluidic convergent nozzles. *Exp. Therm. Fluid Sci.* **166**, 111480 (2025).
2. Peteinaris, A. & Terzis, A. Water-sheet atomization and spray characterization from convergent nozzles. *Phys. Fluids* **37**, 122122 (2025).
3. Ha, B., DePonte, D.P., Santiago, J.G., Device design and flow scaling for liquid sheet jets, Phys. Rev. Fluids 3 (2018) 114202
4. C. J. Crissman et al., Sub-micron thick liquid sheets produced by isotropically etched glass nozzles, Lab. Chip, vol. 22, no. 7, pp. 1365–1373, 2022
5. M. Li, Y. Wu, and Z. Wen, "Estimating surface heat flux of spray cooling by inverse heat-transfer computation and sparse regression," *Int. Commun. Heat Mass Transf.*, vol. 152, p. 107274, 2024,
6. Malinowski, Z., Cebo-Rudnicka, A., Telejko, T., Hadała, B., and Szajding, A. (2015). Inverse method implementation to heat transfer coefficient determination over the plate cooled by water spray. *Inverse Problems in Science and Engineering*, *23*(3), 518–556.